

ENGINEERING IN ADVANCED RESEARCH SCIENCE AND TECHNOLOGY

ISSN 2352-8648 Vol.03, Issue.01 September-2021 Pages: -142-153

BANDWIDTH EFFICIENT NOISE AWARE ACCELERATED IMAGE ENHANCEMENT

¹CHIKKAM SOWBHAGYA LAKSHMI SAI PRIYA, ²S SAMBASIVA RAO DANNINA

¹P.G Student, Dept. of ECE, Prasiddha College of Engineering & Technology, Anathavaram, AP ²Associate Professor, Dept. of ECE, Prasiddha College of Engineering & Technology, Anathavaram, AP

ABSTRACT A novel method of contrast enhancement is proposed for underexposed images, in which heavy noise is hidden. Under low light conditions, images taken by digital cameras have low contrast in dark or bright regions. This is due to a limited dynamic range that imaging sensors have. For these reasons, various contrast enhancement methods have been proposed so far. These methods, however, have two problems: (1) The loss of details in bright regions due to over-enhancement of contrast. (2) The noise is amplified in dark regions because conventional enhancement methods do not consider noise included in images. The proposed method aims to overcome these problems. In the proposed method, a shadow-up function is applied to adaptive gamma correction with weighting distribution, and a denoising filter is also used to avoid noise being amplified in dark regions. As a result, the proposed method allows us not only to enhance contrast of dark regions, but also to avoid amplifying noise, even under strong noise environments. Wavelet transform based fast fractal image coding is proposed and as an extension HAAR wavelet transformation also introduced for further improvement. In this concept, a fractal image compression method based on Haar wavelet method is adopted. To increase the compression gain the indexes of range mean bits have been coded using DWT. Haar wavelet method is more effective then the classical mapping method in compressing color images. The image quality was nearly preserved in comparison with traditional method.

KEYWORDS: De-noising, Wavelet, HAAR, low dynamic range, luminance, Retinex, Shadow-up, weighted variation model.

INTRODUCTION: The low dynamic range (LDR) of modern digital cameras is a major factor preventing them from capturing images as well with human vision. This is due to a limited dynamic range which imaging sensors have. For this reason, images taken by digital cameras have low contrast in dark or bright regions. To overcome the problem, various contrast enhancement methods have so far been proposed[15]. In our previous work[1], we presented a framework of contrast enhancement which can avoid over-enhancement

Copyright @ 2021 ijearst. All rights reserved.
INTERNATIONAL JOURNAL OF ENGINEERING IN ADVANCED RESEARCH
SCIENCE AND TECHNOLOGY

and noise amplification. However, the image enhancement is weak when images include strong noise. Because of this, the result just be enhanced slightly under strong noise environments. The retinex theory allows us to obtain real-world scenes from original images[2] such that color is unaffected by reflection, so we use a control factor based on luminance adaptation to reduce the effect of noise on contrast enhancement. We extend our previous work[1] by applying the retinex theory to achieve a more naturally and clearly enhanced image, even under strong noise environments. to the readily-available cameras on various devices, particularly the cell phones.

PROPOSED METHOD:



Fig1: Proposed block diagram

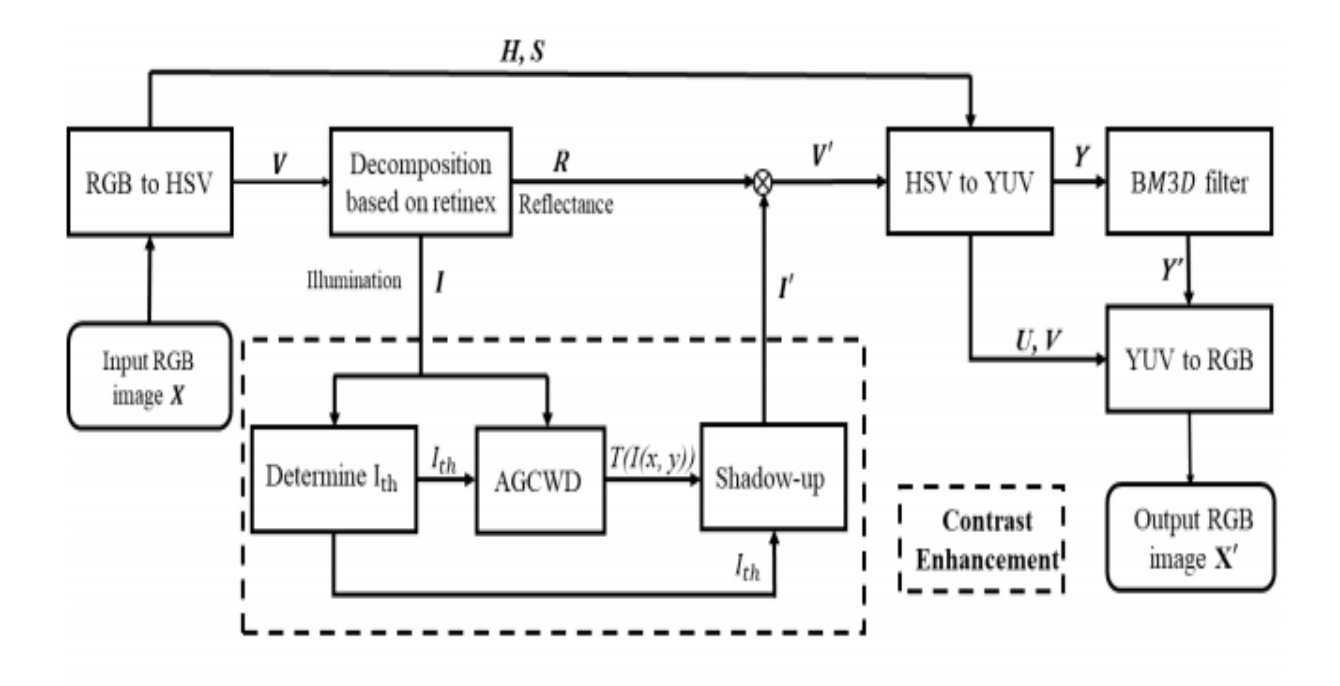


Fig2: Brightness improvement

RETINEX THEORY Retinex theory is based on the relation, $S = R \cdot L$, where original image S is the product of illumination L and reflectance R. When the information of only one surround is used for the conversion of each pixel, its approach is called Single-Scale Retinex (SSR) [6]. In SSR, halo artifacts occur

unnaturally in the boundary of regions with large gradient values. To solve this problem, Multi-Scale Retinex (MSR) [7] was proposed. However, since a logarithmic transformation is used, MSR still causes a problem that the results do not stabilize due to the influence of noise in dark areas. Simultaneous reflection & illumination estimation (SRIE) [8] and weighted variation model (WVM) [1] are also Retinexbased methods. These methods have a good performance for images without noise, but some strange areas are generated in strong noise environments. Therefore, many outstanding methods [2], [9], [10] have been proposed to improve the quality of images, and preserve more details.

WEIGHTED VIBRATIONAL METHOD the proposed model can achieve significant improvement by simply weighting the widely used regularization terms. Compared with classical variational models, the proposed model can preserve the estimated reflectance with more details. Moreover, the proposed model can suppress noise to some extent. An alternating minimization scheme is adopted to solve the proposed model. Experimental results demonstrate the effectiveness of the proposed model with its algorithm. Compared with other variational methods, the proposed method yields comparable or better results on both subjective and objective assessments. The physical model of light reflection can be simply described as $S = R \cdot L$, where S is the observed image, R is the reflectance of the image within the range (0, 1], and L is the illumination within the range $(0, \infty)$. The dot "·" denotes pixel-wise multiplication and all images are vectorized. It follows that $S \le L$. The goal is to estimate the reflectance R and the illumination L from the observed image S. To this end, most variational methods first transform $S = R \cdot L$ into the logarithmic domain, $S = R \cdot L$ where $S = \log(S)$, $S = \log(R)$ and $S = \log(L)$. Using this logarithmic transformation, the first variational algorithm for this decomposition was proposed in [11]. This approach only models the illumination $S = R \cdot L$ and the reflectance $S = R \cdot L$ into the logarithmic of land then estimates the reflectance $S = R \cdot L$ into the logarithmic of land then estimates the reflectance $S = R \cdot L$ into the logarithmic of land then estimates the reflectance $S = R \cdot L$ into the logarithmic of land then estimates the reflectance $S = R \cdot L$ into the logarithmic of land then estimates the reflectance $S = R \cdot L$ into the logarithmic of land then estimates the reflectance $S = R \cdot L$ into the logarithmic of land then estimates the reflectance $S = R \cdot L$ into the logarithmic of land then estimates the reflectance $S = R \cdot L$ into the logarithmic of land then estimates t

AGCWD (ADAPTIVE GAMMA CORRECTION WEIGHTED DISTRIBUTION):

As we know that Power-law transformation (PLT) [2] method, in which main drawback is to give the value of gamma manually for image enhancement. This problem solved by the Adaptive gamma correction weighted distribution method. In which the value of gamma is find out automatically with the help of weighted distribution function. Gamma correction techniques make up a family of general HM (Histogram Modification) techniques obtained simply by using a varying adaptive parameter Y (Gamma). The simple form of the transform-based gamma correction is derived by

 $T(l) = lmax (l / lmax) \Upsilon (1)$

Where lmax is maximum intensity of the input. The intensity l of each pixel in the input image is transformed as T (l) after utilize the Eq. (1). When the contrast is directly or manually modified by gamma correction then different images will results the same changes in intensity as a result of the fixed parameter. So this problem

can be solved by probability density of each intensity level in a digital image can be calculated. As we know that density function of image will be different. So, intensity of each image will be different. The probability density function (pdf) can be approximated by

$$Pdf(l) = n1 / (MN)(2)$$

Where n1 is the number of pixels that have intensity l and MN is total number of pixels in the image. The cumulative distribution function (cdf) is based on pdf, and is formulated as:

Cdf (l) =
$$\sum$$
 pdf (k). (3)

After the cdf of the digital image is obtained from Eq. (3) traditional Histogram Equalization (THE) directly uses cdf as

$$T(l) = cdf(l) lmax. (4)$$

SHADOWUP FUNCTION:

Shadow up function, which consists of a nonlinear part and a linear part, is given by

$$I'(x,y) = \begin{cases} T(I(x,y)) & \text{, if } I(x,y) < I_{th} \\ I(x,y) & \text{, otherwise} \end{cases},$$

where $I(x, y) \in [0, 255]$ is the intensity of illumination layer at a coordinate (x, y), T(I(x, y)) is a monotonically increasing function, and Ith is an upper limit of the nonlinear part for avoiding over enhancement in bright areas. Contrast is enhanced only when I(x, y) is less than the threshold value Ith, according to (1). To determine a proper threshold value Ith for illumination layer, we take into account the luminance distribution of the illumination layer. Let it be $H = \{(x, y) : Ith \le I(x, y) \le Imax\}$, where Ith is the th percentile of luminance I(x, y) of the input image, and Imax is the maximum of I(x, y). The threshold value Ith is calculated as follows:

$$I_{th} = 255 - \frac{1}{|H|} \sum_{(x,y)\in H} I(x,y).$$

A threshold value Ith for a bright image becomes smaller than for a darker image. AGCWD is a method to design a function T(I(x, y)). However, AGCWD usually causes a noise amplification problem, because it does not consider the influence of noise included in images [4]. To overcome this problem, both the Retinex theory and Ith are applied to AGCWD in this paper.

DEOISING FILTER:

Image de-noising has a great tradition in the research field of signal processing because of its fundamental role in many applications. In particular, block-matching and 3D filtering (BM3D) [22] is one of the most successful advances. In this paper, BM3D is used as one of noise suppression techniques. Our purpose is not Copyright @ 2021 ijearst. All rights reserved.

only to enhance contrast with noise suppression, but also to preserve details in bright regions based on Retinex theory. Block-matching and 3D filtering (BM3D) is a 3-D block-matching algorithm used primarily for noise reduction in images.

GROUPING

Image fragments are grouped together based on similarity, but unlike standard k-means clustering and such cluster analysis methods, the image fragments are not necessarily disjoint. This block-matching algorithm is less computationally demanding and is useful later on in the aggregation step. Fragments do however have the same size. A fragment is grouped if its dissimilarity with a reference fragment falls below a specified threshold. This grouping technique is called block-matching, it is typically used to group similar groups across different frames of a digital video, BM3D on the other hand may group macroblocks within a single frame. All image fragments in a group are then stacked to form 3D cylinder-like shapes. The BM3D algorithm has been extended (IDD-BM3D) to perform decoupled deblurring and denoising using the Nash equilibrium balance of the two objective functions.[2]

HAAR WAVELET TRANSFORMATION In this section we shall introduce the basic notions connected with the Haar transform. First, we need to define the type of signals that we shall be analyzing with the Haar transform. Throughout this book we shall be working extensively with discrete signals. A discrete signal is a function of time with values occurring at discrete instants. Generally we shall express a discrete signal in the form f = (f1, f2,...,fN), where N is a positive even integer which we shall refer to as the length of f. The values of f are the N real numbers f1, f2,...,fN. These values are typically measured values of an analog signal g, measured at the time values t = t1, t2,...,tN. That is, the values of f are f1 = g(t1), f2 = g(t2), ..., fN = g(tN). For simplicity, we shall assume that the increment of time that separates each pair of successive time values is always the same. We shall use the phrase equally spaced sample values, or just sample values, when the discrete signal has its values defined in this way. An important example of sample values is the set of data values stored in a computer audio file, such as a .way file. Another example is the sound intensity values recorded on a compact disc. A non-audio example, where the analog signal g is not a sound signal, is a digitized electrocardiogram. Like all wavelet transforms, the Haar transform decomposes a discrete signal into two subsignals of half its length. One subsignal is a running average or trend; the other subsignal is a running difference or fluctuation. Let's begin by examining the trend subsignal. The first trend subsignal, a1 = (a1, a2,...,aN/2), for the signal f is computed by taking a running average in the following way. Its first value, a1, is computed by taking the average of the first pair of values of f: (f1 + f2)/2, and then multiplying it by $\sqrt{2}$. That is, a1 = $(f1 + f2)/\sqrt{2}$. Similarly, its next value a2 is computed by taking the average of the next pair of values of f: (f3 + f4)/2, and then multiplying it by $\sqrt{2}$. That is, $a2 = (f3 + f4)/\sqrt{2}$. Continuing in this way, all of the values of all are produced by taking averages of successive pairs of values of f, and then multiplying these averages by $\sqrt{2}$. A precise formula for the values of all is am = f2m-1 + f2m $\sqrt{2}$, (1.2) for m = 1, 2, 3, ..., N/2. For example, suppose f is defined by eight values, say f = (4, 6, 10, 12, 8, 6, 5, 5); then its first trend subsignal is a1 = $(5\sqrt{2}, 11\sqrt{2}, 7\sqrt{2}, 5\sqrt{2})$. This result can be obtained using Formula (1.2). Or it can be calculated as indicated in the following diagram: f: $46\ 10\ 12\ 86\ 55$ $511\ 75\ \downarrow\downarrow\downarrow\downarrow$ al: $5\sqrt{2}\ 11\sqrt{2}\ 7\sqrt{2}\ 5\sqrt{2}$. You might ask: Why perform the extra step of multiplying by $\sqrt{2}$? Why not just take averages? These questions will be answered in the next section, when we show that multiplication by $\sqrt{2}$ is needed in order to ensure that the Haar transform preserves the energy of a signal. The other subsignal is called the first fluctuation. The first fluctuation of the signal f, which is denoted by d1 = (d1, d2,...,dN/2), is computed by taking a running difference in the following way. Its first value, d1, is calculated by taking half the difference of the first pair of values of f: (f1-f2)/2, and multiplying it by $\sqrt{2}$. That is, $d1 = (f1-f2)/\sqrt{2}$. Likewise, its next value d2 is calculated by taking half the difference of the next pair of values of f: (f3 - f4)/2, and multiplying it by $\sqrt{2}$. In other words, $d2 = (f3 - f4)/\sqrt{2}$. Continuing in this way, all of the values of d1 are produced according to the following formula: dm = $f2m-1 - f2m \sqrt{2}$, (1.3) for m = 1, 2, 3, ..., N/2. For example, for the signal f = (4, 6, 10, 12, 8, 6, 5, 5) considered above, its first fluctuation d1 is $(-\sqrt{2}, -\sqrt{2}, \sqrt{2}, 0)$. This result can be obtained using Formula (1.3), or it can be calculated as indicated in the following diagram: f: 4 6 10 12 8 6 5 5 —1 —1 10 \ $\downarrow \downarrow \downarrow d1: -\sqrt{2} - \sqrt{2} \sqrt{2} 0.$

RESULT:

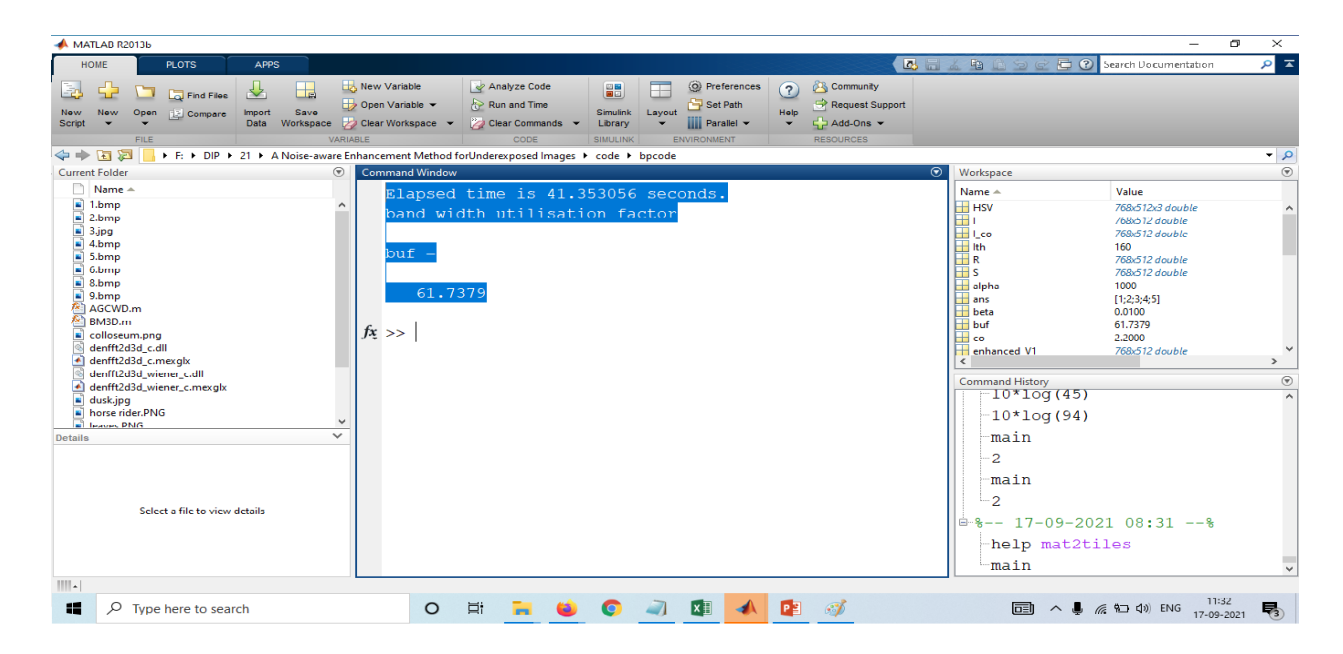


Fig3: Existing performance attribute

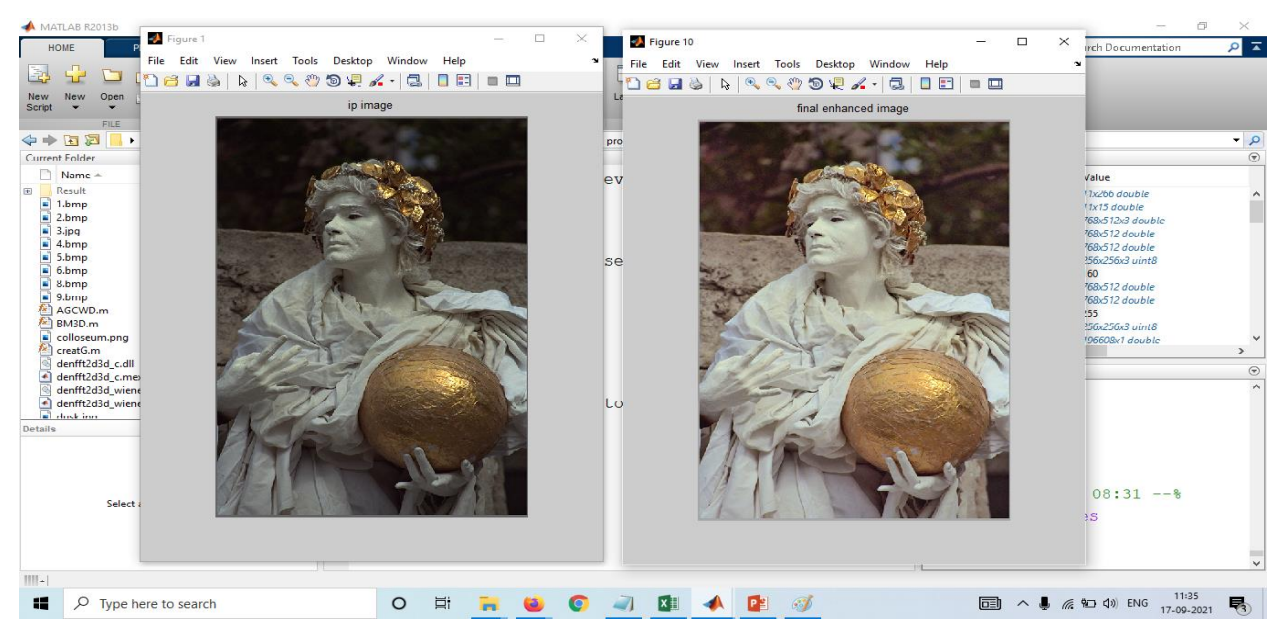


Fig4: Proposed simulation output

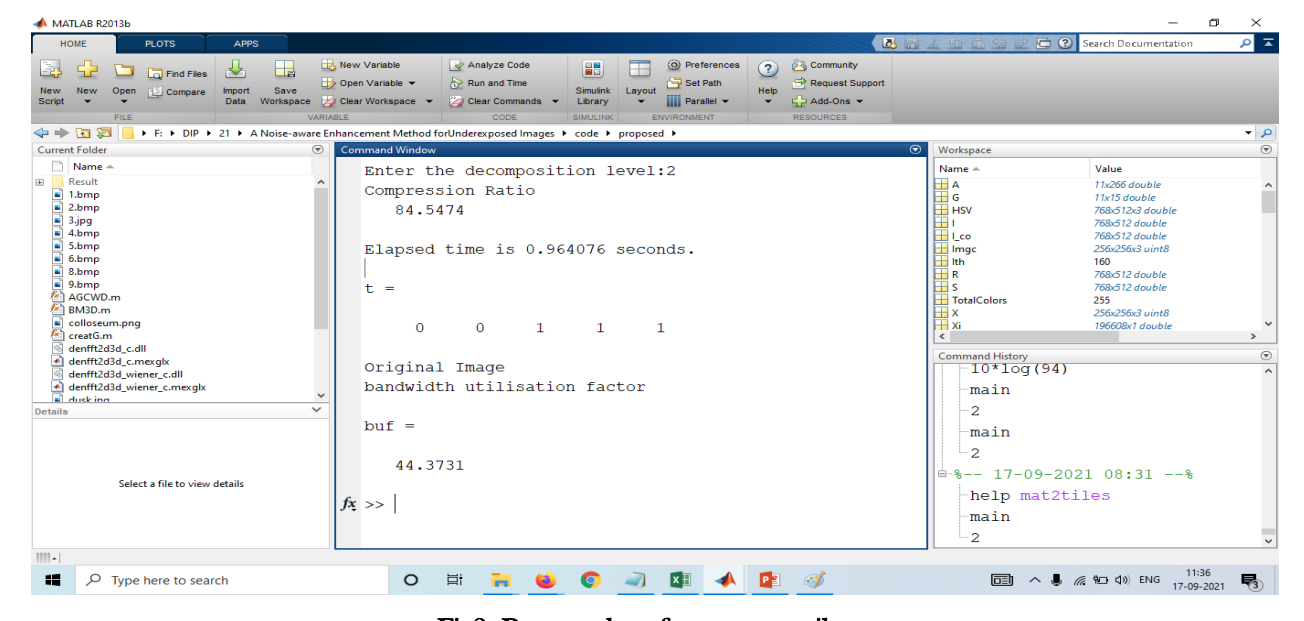


Fig3: Proposed performance attribute

CONCLUSION:

In this paper, we propose and evaluate a visibility estimation framework using multiple image datasets captured by visual systems that provides contextual information that can be used to complement current fog prediction systems. We proposed a novel image contrast enhancement method based on both the Retinex theory and a noise aware shadowup function. The proposed method enhances the contrast of images without Copyright @ 2021 ijearst. All rights reserved.

INTERNATIONAL JOURNAL OF ENGINEERING IN ADVANCED RESEARCH SCIENCE AND TECHNOLOGY

over-enhancement and noise amplification along with low band width utilization ration. Experimental results showed that the proposed method successfully enhances contrast, while preserving details in bright regions and suppressing some noise in dark regions.

FUTURE SCOPE:

So in near future, the problem of uneven illumination of the digital fog removal has to be sorted out. To enhance the visibility of image caused by atmosphere suspended particles like dust, haze and fog which causes failure in image processing such as video surveillance systems, obstacle detection systems, outdoor object recognition systems and intelligent transportation systems. And visibility restoration techniques should be developed to run under various weather conditions.

REFERENCES

- [1] W. Jacobs, V. Nietosvaara, A. Bott, J. Bendix, J. Cermak, M. Silas, and I. Gultepe, "Short range forecasting methods of fog visibility and low clouds," Earth System Science and Environmental Management Final Rep. on COST-722 Action, 2007.
- [2] D. Zhang, E. O'Connor, T. Sullivan, K. McGuinness, F. Regan, and N. E. O'Connor, "Smart multi-modal marine monitoring via visual analysis and data fusion," in Proceedings of the 2nd ACM international workshop on Multimedia analysis for ecological data, pp. 29–34, ACM, 2013.
- [3] D. Zhang, T. Sullivan, C. C. Briciu Burghina, K. Murphy, K. McGuinness, N. E. O'Connor, A. F. Smeaton, and F. Regan, "Detection and classification of anomalous events in water quality datasets within a smart city-smart bay project," International Journal on Advances in Intelligent Systems, vol. 7, no. 1&2, pp. 167–178, 2014.
- [4] S. A. Chatzichristofis and Y. S. Boutalis, "Cedd: color and edge directivity descriptor: a compact descriptor for image indexing and retrieval," in Computer Vision Systems, pp. 312–322, Springer, 2008.
- [5] S. Park, D. Park, and C. Won, "Core experiments on mpeg-7 edge histogram descriptor," MPEG document M, vol. 5984, p. 2000, 2000. [6] J. G. Daugman, "Uncertainty relation for resolution in space, spatial requency, and orientation optimized by two-dimensional visual cortical filters," JOSA A, vol. 2, no. 7, pp. 1160-1169, 1985.
- [7] S. A. Chatzichristofis and Y. S. Boutalis, "Feth: Fuzzy color and texture histogram-a low level feature for accurate image retrieval," in Image Analysis for Multimedia Interactive Services, 2008. WIAMIS'08. Ninth International Workshop on, pp. 191–196, IEEE, 2008.
- [8] K. E. Van De Sande, T. Gevers, and C. G. Snoek, "Evaluating color descriptors for object and scene recognition," Pattern Analysis and Machine Intelligence, IEEE Transactions on, vol. 32, no. 9, pp. 1582–1596, 2010.

- [9] G. Pass and R. Zabih, "Comparing images using joint histograms," Multimedia systems, vol. 7, no. 3, pp. 234–240, 1999.
- [10] J.-R. Ohm, L. Cieplinski, H. J. Kim, S. Krishnamachari, B. Manjunath, D. S. Messing, and A. Yamada, "The mpeg-7 color descriptors," Introduction to MPEG-7: Multimedia Content Description Interface, Wiley, 2001.
- [11] J. Hafner, H. S. Sawhney, W. Equitz, M. Flickner, and W. Niblack, "Efficient color histogram indexing for quadratic form distance functions," Pattern Analysis and Machine Intelligence, IEEE Transactions on, vol. 17, no. 7, pp. 729–736, 1995.
- [12] H. Tamura, S. Mori, and T. Yamawaki, "Textural features corresponding to visual perception," Systems, Man and Cybernetics, IEEE Transactions on, vol. 8, no. 6, pp. 460–473, 1978.
- [13] B. E. Boser, I. M. Guyon, and V. N. Vapnik, "A training algorithm for optimal margin classifiers," in Proceedings of the fifth annual workshop on Computational learning theory, pp. 144–152, ACM, 1992.
- [14] M. Sonka, V. Hlavac, and R. Boyle, Image processing, analysis, and machine vision. Cengage Learning, 2014.
- [15] C.-C. Lin, S.-H. Chen, T.-K. Truong, and Y. Chang, "Audio classification and categorization based on wavelets and support vector machine," Speech and Audio Processing, IEEE Transactions on, vol. 13, no. 5, pp. 644–651, 2005.
- [16] T. Joachims, Text categorization with su pport vector machines: Learning with many relevant features. Springer, 1998.
- [17] C.-W. Hsu, C.-C. Chang, C.-J. Lin, et al., "A practical guide to support vector classification," 2003
- [18] Q. Ji and X. J. Yang, "Real-time eye, gaze, and face pose tracking for monitoring driver vigilance," *Real-time Imaging*, vol. 8, no. 5, pp. 357–377, 2002.
- [19] L. Bretzner and M. Krantz, "Towards low-cost systems for measuring visual cues of driver fatigue and inattention in automotive applications," *Vehicular Electronics and Safety. IEEE International Conference*, pp. 161–164, 2005.
- [20] J. Heinzmann, D. Tate, and R. Scott, "Using technology to eliminate drowsy driving," *SPE International Conference on Health, Safety, and Environment in Oil and Gas Exploration and Production*, April 2008.
- [21] "Smart eye," http://www.smarteye.se.
- [22] "Seeingmachines," http://www.seeingmachines.com.
- [23] J. Bos, W. Bles, and E. Groen, "A theory on visually induced motion sickness," *Displays*, vol. 29, no. 2, pp. 47–57, 2008.
- [24] T. "Akerstedt, B. Peters, A. Anund, and G. Kecklund, "Impaired alertness and performance driving home from the night shift: a driving simulator study," *Journal of Sleep Research*, vol. 13, no. 1, pp. 17–20.
- [25] "Tutor [online]," http://www.landersimulation.com/index.php.

- [26] B. Lang, A. Parkes, S. Cotter, R. Robbins, C. Diels, P. Vanhulle, G. Turi, E. Bekiaris, M. Panou, and J. K. . S. Poschadel, "Train-all integrated system for driver training and assessment using interactive education tools and new training curricula for all modes of road transport," 2007.
- [27] N. Stanton, P. Salmon, G. Walter, and C. B. . D. Jenkins, "Human factors methods: A practical guide for engineering and design," 2005.
- [28] K. Kaida, M. Takahashi, T. Akerstedt, A. Nakata, Y. Otsuka, and T. H. . K. Fukasawa, "Validation of the karolinska sleepiness scale against performance and eeg variables."
- [29] P. Viola and M. J. Jones, "Robust real-time face detection," *Int. J. Comput. Vision*, vol. 57, no. 2, pp. 137–154, 2004.